IOPscience iopscience.iop.org

Home Search Collections Journals About Contact us My IOPscience

Selective electron spin resonance measurements of micrometer-scale thin samples on a substrate

This content has been downloaded from IOPscience. Please scroll down to see the full text.

2013 Meas. Sci. Technol. 24 115009

(http://iopscience.iop.org/0957-0233/24/11/115009)

View the table of contents for this issue, or go to the journal homepage for more

Download details:
This content was downloaded by: aharonblank
IP Address: 132.68.67.215
This content was downloaded on 10/10/2013 at 06:43

Please note that terms and conditions apply.

Meas. Sci. Technol. **24** (2013) 115009 (7pp) doi:10.1088/0957-0233/24/11/115009

Selective electron spin resonance measurements of micrometer-scale thin samples on a substrate

Ekaterina Dikarov[1], Matthias Fehr[2], Alexander Schnegg[2], Klaus Lips[2] and Aharon Blank[1,3]

[1] Schulich Faculty of Chemistry, Technion–Israel Institute of Technology, Haifa 32000, Israel
[2] Helmholtz-Zentrum Berlin für Materialien und Energie, Institut für Silizium-Photovoltaik, Kekuléstr. 5, D-12489 Berlin, Germany

E-mail: ab359@tx.technion.ac.il.

Received 3 June 2013, in final form 13 August 2013
Published 9 October 2013
Online at stacks.iop.org/MST/24/115009

Abstract
An approach to the selective observation of paramagnetic centers in thin samples or surfaces with electron spin resonance (ESR) is presented. The methodology is based on the use of a surface microresonator that enables the selective obtention of ESR data from thin layers with minimal background signals from the supporting substrate. An experimental example is provided, which measures the ESR signal from a 1.2 μm polycrystalline silicon layer on a glass substrate used in modern solar-cell technology. The ESR results obtained with the surface microresonator show the effective elimination of background signals, especially at low cryogenic temperatures, compared to the use of a conventional resonator. The surface microresonator also facilitates much higher absolute spin sensitivity, requiring much smaller surfaces for the measurement.

Keywords: ESR, EPR, thin paramagnetic layer

(Some figures may appear in colour only in the online journal)

1. Introduction

Modern science and technology are often involved in the fabrication and use of thin layers, such as molecular monolayers, metallic and dielectric depositions with nanometer-scale thickness, submicrometer- and micrometer-scale semiconductors, oxides and many more. These thin layers can be characterized by a wide array of morphological, chemical and physical tools. One important aspect of many of these structures is the paramagnetic properties of the layer, namely, the existence of unpaired electron spins, their concentration, spatial distribution and microenvironment. Examples of systems for which paramagnetic properties are of paramount importance are: defects, impurities and dopants in semiconductors [1]; defects and impurities in oxides [2]; paramagnetic molecular monolayers [3]; and native surface defects, vacancies and dangling bonds [4]. The measurement and characterization of the paramagnetic properties of such solid-state samples is usually carried out by means of electron spin resonance (ESR) spectroscopy [5, 6]. When compared to some surface characterization techniques, such as x-ray photoelectron spectroscopy (XPS) and secondary ion mass-spectrometry (SIMS), the spatial resolution of ESR is found to be comparable and many times even better [7]. However, compared to most other surface techniques (e.g., STM, AFM, capacitance and photo luminance methods), the sensitivity and spatial resolution of ESR are relatively low, which greatly limits the measurements of surface or thin layer samples [3, 8, 9]. For example, commercial systems reach sensitivity levels of $\sim 10^9$ spins/$\sqrt{\text{Hz}}$ at best [10]. This sensitivity limitation also affects the available imaging resolution of heterogeneous samples, which in commercial systems reaches $\sim$25 μm [11]. This is because, as the image's voxel size decreases, it contains less and less spins and thus quickly

[3] Author to whom any correspondence should be addressed.

 © 2013 IOP Publishing Ltd Printed in the UK & the USA

runs into the sensitivity limitation 'wall'. For these reasons, thin layered samples pose some of the greatest challenges to modern ESR capabilities: (*a*) they have a small number of spins and (*b*) their signal often needs to be separated from the support matrix or substance on which they are placed.

The first concern can sometimes be dealt with by measuring several layers stacked together in order to increase sensitivity [3, 12, 13]. However, this does not solve the second concern of separating signals between the layer and its support. In some cases, especially sensitive forms of detection, such as electrically detected magnetic resonance (EDMR), can be used in thin semiconducting layers or in thin-film devices to increase sensitivity and obtain signals only from defect spin or conduction electron spin states [14]. However, these and other specialized detection methods (like MRFM [15] and STM–ESR [16]) can be employed solely on very specific types of samples, under specific conditions, and can be thus considered only as a very partial solution to these problems. High-resolution ESR microimaging [7] may be one possible alternative, with the thin layer and substrate being spatially separated during the imaging process. However, this approach greatly complicates the measurement procedure and can be found only in specialized laboratories (see [7]). Furthermore, it faces the significant problem of aligning the gradient axis exactly perpendicular to the sample plane to properly separate it from the background support during imaging. Another possible approach to the selective measurement of thin samples makes use of surface resonators, where the microwave (MW) magnetic field component (B_1) is confined to a short distance from the surface. Such resonators have recently been developed by several groups [17–19], but were not tested against the problem of selective measurements of thin layers supported by a substrate containing paramagnetic centers.

In this work we show that it is possible to provide a generic solution to the above-mentioned problems using a unique type of miniature surface loop-gap microresonator recently developed by us. Specifically, the surface resonator makes it possible to obtain sufficient ESR signals from a relatively very small number of electron spins in a thin paramagnetic sample with minimal interference from its substrate, which normally would have contributed strong background signals with a broad spectrum. We provide an experimental example of this by measuring paramagnetic defects in a 1.2 μm thick layer of polycrystalline silicon deposited on glass (the latter showing strong background signals at low temperatures)—a configuration that is used in modern solar-cell technology.

2. Experimental methods

In this work we employed two types of spectrometers. One of them is a conventional Bruker E580 X-Band EPR system that includes a standard ER 4118X-MD5 dielectric resonator with an inner diameter of 5 mm (situated at the Helmholtz Zentrum Berlin) and the other is a 'home-made' system constructed and operated at the Technion in Haifa. The latter system was described in detail in [20] and the referenced documents therein. In brief, it is a home-made pulsed system operating at 6–18 GHz (extendable to 33–37 GHz), capable also of imaging heterogeneous samples. The heart of the system and of this experiment is the unique surface loop-gap microresonator shown in figures 1(*a*) and (*b*) [7]. In previous reports we have provided information about the design approach and fabrication method of this resonator, and also its capability to focus the magnetic microwave field on a small two-dimensional (2D) volume [7, 19, 21]. Reference [19] provides details about the three-dimensional spatial variation of the microwave magnetic field for the type of surface resonator employed in this work. Here, however, we are mainly interested in making use of the fast out-of-plane decay of the field, as depicted in figure 1(*c*). It is clear that within the first 10 μm the field drops to ~40% of its initial value in the plane, which means that the ESR signal drops by a factor of ~6 (proportional to $B_1{}^2$). The resonator is placed in a cryostat whose details were provided elsewhere [7], enabling us to measure ESR signals in the temperature range of 3–300 K. This capability is important in order to demonstrate the usefulness of our approach to selective surface measurement because, in many cases, substrates that have impurities produce strong and broad background signals, especially at low cryogenic temperatures.

The sample used in our experiments is a polycrystalline silicon layer (thickness: 1.2 μm) produced by solid-phase crystallization of electron-beam evaporated amorphous silicon on a Corning Eagle XG glass substrate (thickness: 1.1 mm). Figure 2 shows the sample on our surface resonator (photo). The sample's size is either ~1.5 mm × 1.5 mm (used with the surface resonator) or ~4 mm × 4 mm (with the conventional resonator). The spin concentration of this sample was measured using X-Band CW ESR and was found to be ~9×10^{17} spins cm^{-3}. Notice that the resonator's orientation with respect to the microstrip line can be either with the gap along the line (as in figure 1) or perpendicular to it (as in figure 2). Both configurations are possible, but require slightly different relative positions between the resonator and the microstrip line for achieving optimal coupling. Since the static field in our set-up is always along the microstrip line, it means that the microwave magnetic field component produced by the resonator along the line would not contribute to ESR signal excitation and detection. Thus, switching between the two different relative orientations enhances the contribution of one in-plane microwave magnetic field component over the other, but apart from this the choice of the specific relative orientation in a given experiment is thus quite arbitrary.

3. Results and discussion

The problem of substrate paramagnetic background signals is easily observable when measuring our sample using the conventional Bruker system. Figure 3(*a*) shows typical CW–ESR measurements of the polycrystalline silicon-on-glass sample, carried out at 10 K. It is clear that a complete hodgepodge of signals appears, of which only the central one ($g = 2.0054$, width of ~7.6 G) is due to our thin sample of interest. This signal is attributed, through its g-value and linewidth, to the dangling bonds at the interface

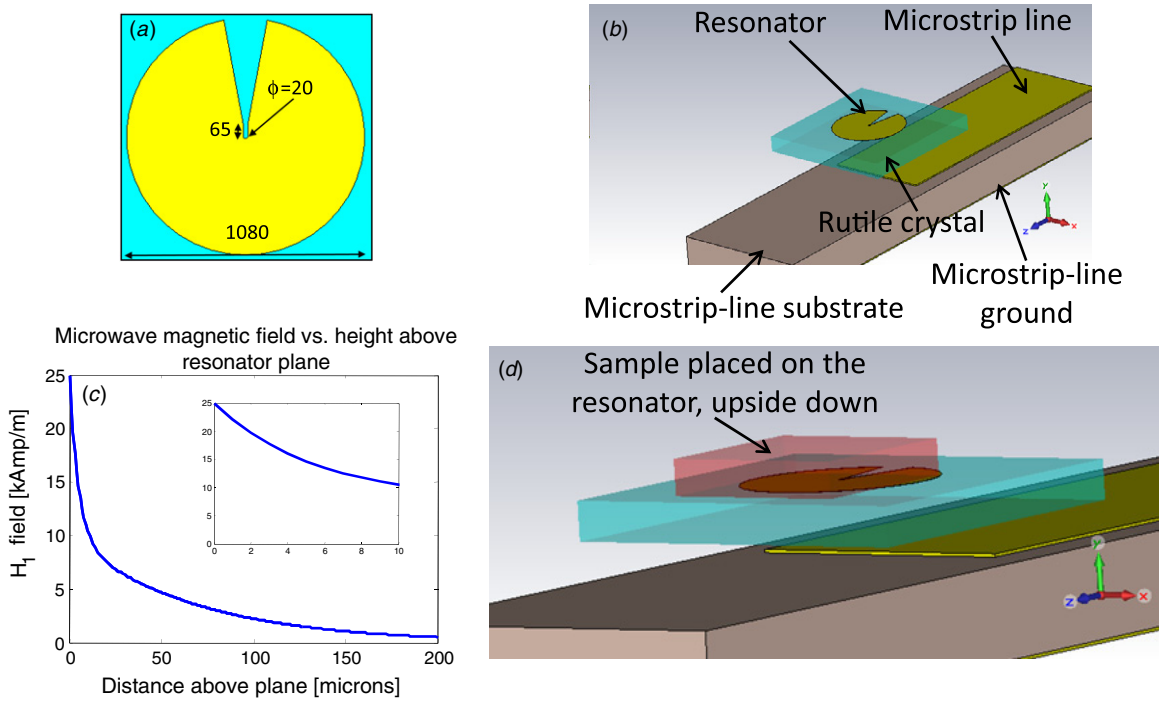

Figure 1. The surface loop-gap microresonator used in some of our experiments. It is made of a 1 μm copper layer, deposited on a 200 μm thick single crystal of rutile. (*a*) Top view of the resonator, showing its dimensions in micrometers. (*b*) Drawing showing the coupling method of the resonator to a microstrip line. (*c*) The microwave magnetic field as a function of distance from the surface of the resonator. The insert shows the first 10 μm in detail. The field profile decay was calculated with CST Microwave Studio finite element software when there was no sample on the resonator (simply air). Upon placing a 1 μm Si sample (permittivity of $\sim$11) backed by thick glass (permittivity of $\sim$4.7), the calculated field decay profile changed very slightly and is almost indistinguishable from the one without the sample. However, thick materials with larger permittivity ($>$20) would result in more moderate out-of-plane field decay. (*d*) Close-up view of the resonator and the microstrip feed line, with a thin sample placed on top of the resonator for ESR measurements.

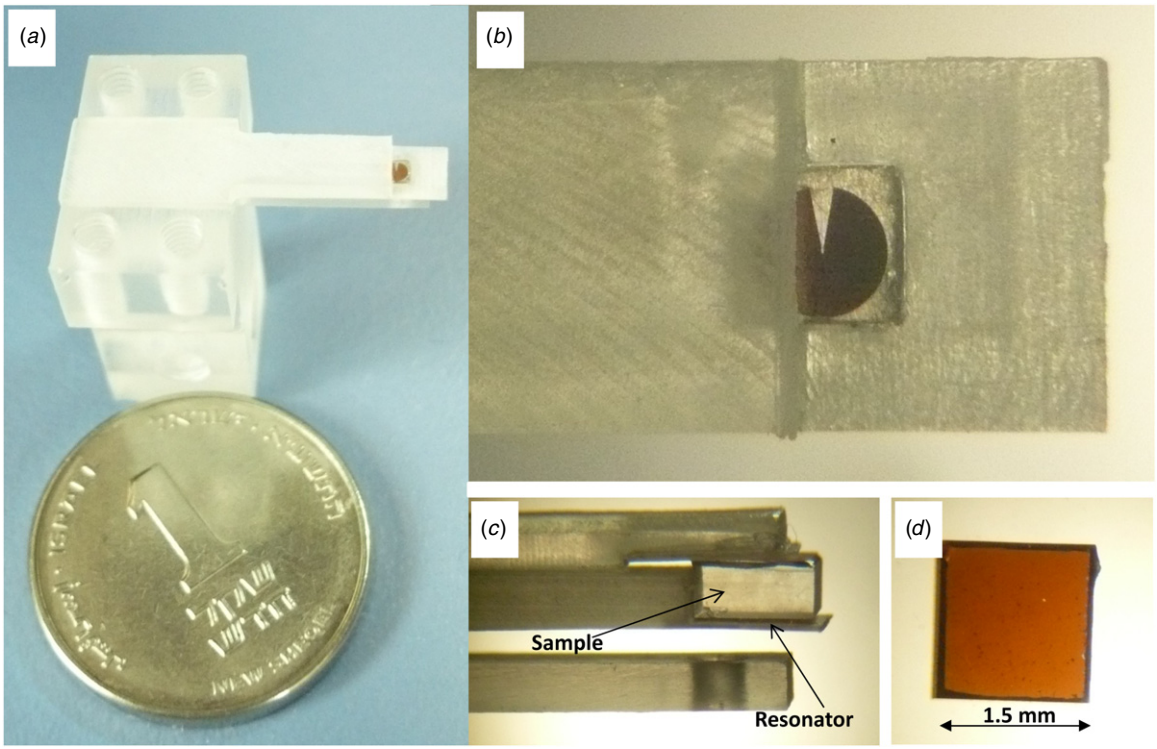

Figure 2. Photos of the resonator and the polycrystalline silicon sample. (*a*) The resonator held with a Rexolite holder, near a standard 1-Israeli-shekel coin (diameter 18 mm). (*b*) The resonator under the microscope. (*c*) Side view of the resonator with the sample placed on it. (*d*) The polycrystalline silicon sample.

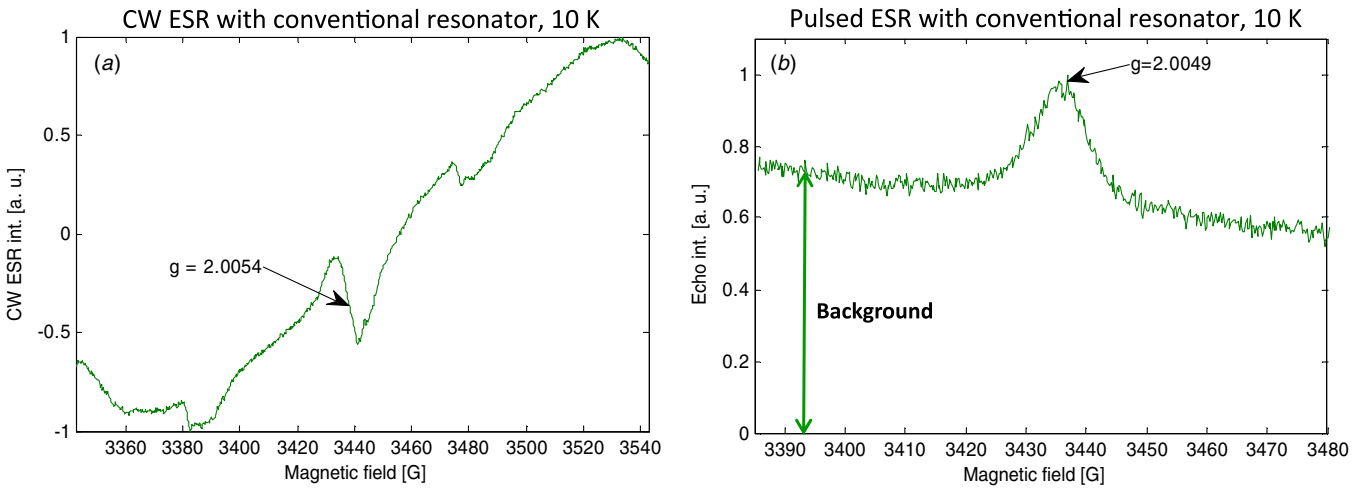

Figure 3. X-band CW and pulsed ESR spectra of the polycrystalline silicon sample measured using the conventional resonator. (*a*) CW spectrum measured at 10 K and 9.646 GHz. Measurement parameters are: microwave power of 0.2 mW; modulation amplitude of 3G; modulation frequency of 10 kHz; time constant of 20.48 ms; and 10 averaging scans. (*b*) Field-swept primary spin-echo spectrum measured at 10 K by the Bruker system using a microwave power of 100 W that employs a 16 ns $\pi/2$ pulse and two-step phase cycling. Additional measurement parameters are: interpulse delay of $\tau = 300$ ns, repetition time of 81.6 ms and averaging over 1000 shots per field point.

(grain boundary) between the crystals of the thin silicon layer [13, 22]. The rest of the signals originate in defects and paramagnetic impurities of the supporting glass substrate. The broad background signals are not seen in similar experiments where the silicon layer is removed from the glass [13]. Background signals can sometimes be separated according to their relaxation properties, so that if their T_2 is much shorter than the signal of interest they would not be seen in echo experiments. However, the field-swept primary echo results provided in figure 3(*b*) clearly show that some of the background problem persists even in pulsed acquisition. The 'bump' on the broad background is clearly identified as the signal from the dangling bond defects through its *g*-value and its full width half maximum linewidth, $\Delta B_{1/2} = 12.5$ G, which corresponds well to the peak-to-peak linewidth, $\Delta B_{pp} = 7.6$ G measured in CW mode (the ratio between $\Delta B_{1/2}$ obtained in pulsed mode to ΔB_{pp} is known to vary between ~ 1.2 and 1.7, depending on the exact line shape [23]).

The high level of background signals affects the capability to spectroscopically characterize the paramagnetic species in the thin layer, especially when the thin layer of interest itself also has broad signals. For example, figure 3 does not allow one to determine *a priori* whether or not the background signal is due to the sample. One possible way to overcome this is by physically separating the thin sample from the substrate, as can be achieved to some extent with the poly-silicon sample using adhesive tape [13]. However, in the general case of thin samples on a thick substrate, this may not be a valid option. Background signals can interfere also with simple measurements of the relaxation times (T_1 and T_2), which may face substantial difficulties due to signal overlap (see table 1). As a consequence, we could not obtain a fit to the T_1 value at 10 K, where the decay signal is characterized by several and very different types of contributions from the sample and the substrate. We did obtain a reasonable fit to T_2, but it is probably a mixture of similar T_2 values of the sample and substrate (that occur by chance in this case).

The alternative approach offered here to the unobstructed observation of thin samples on a substrate involves the use of our surface loop-gap microresonator. In this method, the sample is placed face-down on the resonator (figures 1(*d*) and 2(*c*)). Due to the fast decay of the microwave magnetic field when going out of the resonator's plane, most of the signal comes from the volume close to the surface of the sample, meaning mainly from the thin layer and much less from the thick substrate. Figure 4 shows the field-swept Hahn echo data for a single polycrystalline silicon-on-glass sample measured at 80 and 10 K. The experimental parameters at 80 K (10 K) were: repetition rate of 5 kHz (200 Hz), 12 000 (2000) averages per field point, sweep resolution of 1 Gauss, $\tau = 500$ ns, and pulse lengths of $p_1 = 30$ ns and $p_2 = 60$ ns. All measurements used eight-step phase cycles (CYCLOPS and $\pm$ on the first pulse). The *g*-factor at the center of the line is 2.0055, similar to the one measured using the conventional resonator, but the linewidth is a bit broader ($\Delta B_{1/2} = 14.2$ G), possibly due to the higher static field employed. Thus, it is apparent that at both temperatures the surface resonator measures the same dangling bond spectrum as measured by the conventional Bruker CW and pulsed system employing a conventional resonator. The difference, however, is a much smaller background signal obtained with the surface resonator, especially when comparing the two types of approaches at 10 K. We have found that this background signal is seen as a regular echo in the time domain trace (not shown), goes away only when the field is turned off or swept $\sim$2–3 kG away from resonance, and thus is not the result of some microwave ring-down due to transient excitation pulses. The background signal in surface resonator measurements can be enhanced by increasing the MW excitation power (figure 4(*b*), red curve). This is because the excitation of deeper parts of the sample becomes more efficient and the large volume of the substrate starts to contribute substantially to the ESR signal. Due to the highly inhomogeneous B_1 of the resonator when going out-of-plane it is not possible to obtain a proper

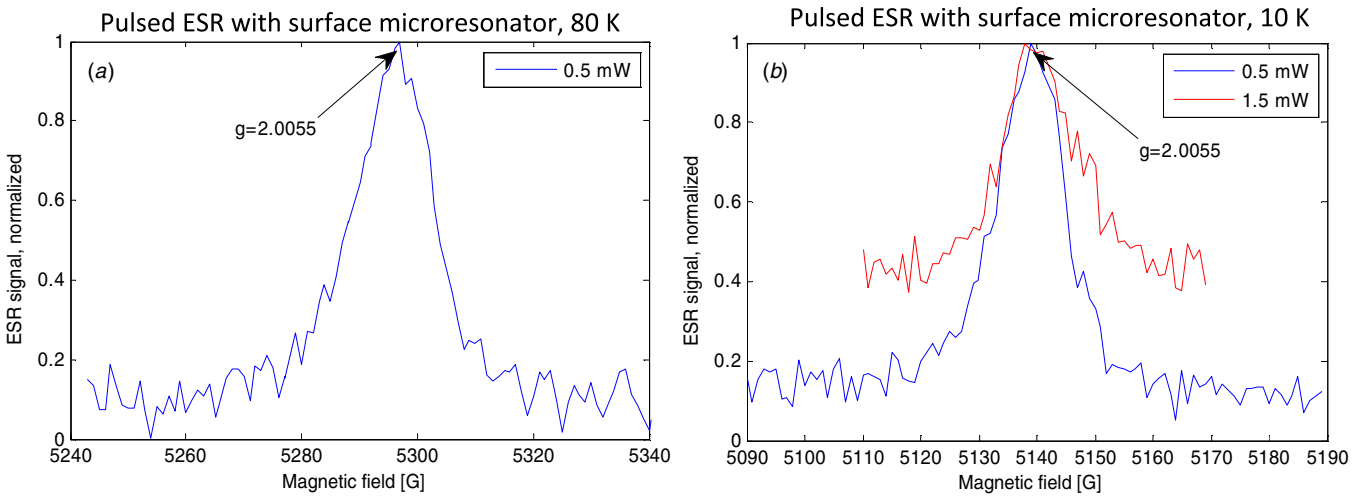

Figure 4. Field-swept echo spectra for the polycrystalline silicon sample, measured by the surface loop-gap microresonator (*a*) at 80 K and at a frequency of 15.081 GHz and (*b*) at 10 K and 14.625 GHz with two different MW power levels (0.5 mW—blue, 1.5 mW—red). Signal amplitude is normalized.

Table 1. Relaxation times of a polycrystalline silicon sample on glass measured by a conventional and a surface resonator. T_1 values were measured in the conventional resonator using an inversion recovery technique, and in the surface resonator using the saturation recovery method. T_2 values were measured by both resonators using a Hahn echo sequence with stepping of the interpulse distance, τ.

	T_1 (95% confidence interval)	T_2 (95% confidence interval)
10 K conventional resonator	Fit could not be obtained	1.35 (1.33, 1.37) μs
10 K surface resonator	10.7 (5.2, 14.3) ms	1.54 (1.23, 1.91) μs
80 K conventional resonator	120.1 (116.5, 123.6) μs	0.76 (0.74, 0.78) μs
80 K surface resonator	119.0 (110.2, 130.1) μs	1.07 (0.65, 2.03) μs

nutation curve for the thin sample of the thick substrate. Therefore, the most optimal way to acquire the signal is to employ the smallest MW power that still provides enough ESR signal from the thin sample, thereby minimizing the background-signal contribution. In addition to the obvious spectroscopic advantages of using selective excitation, the low level of background signal also enables a much better fit to the measured relaxation data, which can be better described by a single ESR species (table 1). The values obtained at 10 K with the surface resonator are comparable to those appearing in the literature for dangling bonds in bulk amorphous silicon with similar defect concentrations [24].

Based on figures 3 and 4, it is clear that the surface microresonator exhibits a very good capability to selectively measure the signal from a thin paramagnetic layer, situated on a substrate that by itself gives a strong paramagnetic signal at low temperatures. Both resonators measured the same sample signal, as verified by its g-factor and linewidth; however, in the conventional-resonator measurement, a strong background signal almost 'swamps' the thin layer signal. The T_2 results obtained from both resonators are very similar (table 1) at 80 and 10 K, most probably because the background signal from the substrate has a similar T_2 as that of the thin sample of interest. The confidence intervals of the T_2 (and T_1) results of the surface resonator are worse than those of the conventional resonator (in cases where fitting was achievable), because with the former we typically measured only 12 points in the decay curve (as compared to hundreds of point in the Bruker system), due to our (current) software constraints. This can be corrected in the future by employing improved software in order to acquire more points. In this work, the conventional resonator failed to obtain a good spectrum and a good fit to the T_1 value only at 10 K. However, this is just the tip of the iceberg, since the general problem of background signals with thin layers becomes much more severe when dealing with even thinner layers having smaller spin concentrations, and at medium-to-low cryogenic temperatures.

In addition to its surface selectivity, the microresonator is also much more sensitive as applied to measurements of small numbers of spins, which is of importance for size-limited samples. In the present experimental example, the resonator obtains most of its signal from a surface area of $\sim$20 μm $\times$ 65 μm [7], which means that the total number of spins measured is $\sim 9 \times 10^{17}$ spins cm^{-3} $\times$ 20 μm $\times$ 65 μm $\times$ 1.2 μm $= 1.4 \times 10^9$ spins. The signal-to-noise ratio (SNR) obtained ($\sim$10–20, depending on temperature) is comparable to the one measured using the conventional resonator on a sample having $\sim$12 300 times more spins (since the size of the sample used with it is $\sim$4 mm $\times$ 4 mm). In more quantitative terms, the absolute spin sensitivity of the surface resonator employed here is $\sim 12\,300/\sqrt{(12\,000/1000)} = 3550$ times better than that of the conventional resonator, taking into account the larger number of averages used for the surface resonator measurements (12 000 compared to 1000 in the conventional resonator, as reflected by the square root factor in the expression). It should also be noted that a small part of this improved sensitivity (approximately a factor of 2) results from the surface resonator

system being operated at a slightly higher static field than the Bruker system.

The expected absolute spin sensitivity of the surface resonator can be estimated for this type of sample (with its measured T_1 and T_2 values, as provided in table 1), using the expressions and data in [7, 21], to be $\sim 6 \times 10^6$ spins/$\sqrt{\text{Hz}}$ at 80 K and $\sim 1 \times 10^6$ spins/$\sqrt{\text{Hz}}$ at 10 K (for SNR = 1). Given the SNR we obtained in the measured traces (~10–20, see figure 4), with approximately a few seconds of averaging per point, and the estimated number of spins in the resonator ($\sim 1.4 \times 10^9$), this theoretical prediction seems to be too optimistic. However, factors such as partial excitation of broad inhomogenous lines, T_2 relaxation and heterogeneous sensitivity within the resonator volume, were not considered in the spin sensitivity theory and, when accounted for, they bring the estimation much closer to the values measured by us. Another important issue to be emphasized is that the pulsed experiment with the microresonator requires a power of only ~0.5 mW to efficiently excite the spins on the surface, compared to hundreds of watts in a conventional resonator. This is because the surface resonator has a microwave magnetic field conversion factor of ~ 135 G/$\sqrt{\text{W}}$ (based on a $\pi/2$ pulse of 30 ns with power of 0.5 mW—see also [21]), while the conventional rectangular resonator has a conversion factor of only ~ 0.55 G/$\sqrt{\text{W}}$.

At this point it is important to consider what would be the most optimal resonator for measuring thin samples and obtaining the best SNR. This depends on whether or not the size of the surface is a limitation. In order to analyze this problem, it is possible to use the expression for SNR for a point-like sample with a small volume V_v situated in a resonator with effective volume V_c, which is proportional to [7]

$$\text{SNR} \propto \frac{MV_V\sqrt{Q_u}}{\sqrt{V_c}}, \tag{1}$$

where M is proportional to the sample's spin concentration and Q_u is the unloaded quality factor of the resonator. This expression clearly shows that for a size-limited (zero-dimensional) sample (where V_v is constant and much smaller than V_c) it is best to employ the smallest possible resonator while still trying to maintain good Q values, of course.

In the case that the sample completely fills the resonator, the SNR of all individual point-like samples can be integrated ($V_v \sim V_c$) in order to obtain SNR $\propto M\sqrt{V_c}\sqrt{Q_u}$. Thus, for large volumetric samples it is clearly best to use the largest available resonator while still maintaining high Q values (assuming there is enough power for a pulsed operation). For a two-dimensional sample with thickness δ the situation is a bit more complicated. If we assume a resonator with typical dimensions of a in the surface and b out of surface, we obtain the following after integrating the point-like sample expression in equation (1):

$$\text{SNR} \propto \frac{Ma^2\delta\sqrt{Q_u}}{\sqrt{a^2b}} = \frac{Ma\delta\sqrt{Q_u}}{\sqrt{b}} \tag{2}$$

This means that for a conventional resonator in which $a \approx b \gg \delta$, the SNR $\propto M\sqrt{a}\delta\sqrt{Q_u}$, which means that SNR-wise it is still best to use the largest possible resonator, even for two-dimensional thin samples. It is also clear from equation (2) that it is best to minimize b—optimally reaching a thickness of just δ, which allows us to obtain the best SNR for a two-dimensional sample: SNR $\propto Ma\sqrt{\delta}\sqrt{Q_u}$. The design and construction of such an almost purely two-dimensional resonator is of course a considerable challenge, but one which we have already started to pursue. This would be the optimal solution for measuring most thin or surface samples that in many cases are not limited in size (at least within a few millimeters).

In summary, we have shown that miniature surface resonators provide enhanced selectivity over conventional volume resonators for ESR spectroscopy on thin layers. This high selectivity of the surface resonator is demonstrated experimentally on a polycrystalline silicon layer designed for applications in thin-film silicon solar cells. ESR signals from the glass substrate are drastically reduced in intensity when using a surface resonator. Surface resonators are also shown to be characterized by a much higher absolute spin sensitivity, which is of advantage in size-limited samples, but for large 2D samples it is shown that better sensitivity is obtained using conventional volume resonators. Future designs of large-area 2D surface resonators should provide the best of both worlds, meaning having both high selectivity and also high spin concentration sensitivity, which is useful when sample area is not a limitation.

Acknowledgments

This work was partially supported by grant #G-1032-18.14/2009 from the German–Israeli Foundation (GIF), grant #213/09 from the Israeli Science Foundation, grants #201665 and #309649 from the European Research Council (ERC), and by the Russell Berrie Nanotechnology Institute at the Technion. AS received funding from the German Federal Ministry of Education and Research (BMBF grant #03SF0328). Dr Tobias Sontheimer and Stefan Common (HZB) are gratefully acknowledged for the production of the polycrystalline silicon samples.

References

[1] McCluskey M D and Haller E E 2012 *Dopants and Defects in Semiconductors* (Boca Raton, FL: Taylor and Francis)

[2] Barklie R C, Collins M, Richardson M and Borde I 2001 An electron paramagnetic resonance study of defects in PECVD silicon oxides *J. Mater. Sci., Mater. Electron.* **12** 231

[3] Mannini M, Rovai D, Sorace L, Perl A, Ravoo B J, Reinhoudt D N and Caneschi A 2008 Patterned monolayers of nitronyl nitroxide radicals *Inorg. Chim. Acta* **361** 3525

[4] Thompson T L and Yates J T 2005 TiO_2-based photocatalysis: surface defects, oxygen and charge transfer *Top. Catal.* **35** 197

[5] Misra S K (ed) 2011 *Multifrequency Electron Paramagnetic Resonance, Theory and Applications* (Berlin: Wiley-VCH)

[6] Wurz R, Meeder A, Marron D F, Schedel-Niedrig T, Knop-Gericke A and Lips K 2004 Native oxidation of $CuGaSe_2$ crystals and thin films studied by electron paramagnetic resonance and photoelectron spectroscopy *Phys. Rev.* B **70** 205321

[7] Twig Y, Dikarov E and Blank A 2012 Cryogenic electron spin resonance microimaging probe *J. Magn. Reson.* **218** 22

[8] Fanciulli M, Bonera E, Carollo E and Zanotti L 2001 EPR and UV-Raman study of BPSG thin films: structure and defects *Microelectron. Eng.* **55** 65
[9] Fanciulli M, Bonera E, Nokhrin S and Pacchioni G 2006 Phosphorus–oxygen hole centers in phosphosilicate glass films *Phys. Rev.* B **74** 134102
[10] Schmalbein D, Maresch G G, Kamlowski A and Hofer P 1999 The Bruker high-frequency-EPR system *Appl. Magn. Reson.* **16** 185
[11] Bruker 2010 EPR news letter *EPR News Lett.* **2010** 18
[12] Ruthstein S, Artzi R, Goldfarb D and Naaman R 2005 EPR studies on the organization of self-assembled spin-labeled organic monolayers adsorbed on GaAs *Phys. Chem. Chem. Phys.* **7** 524
[13] Fehr M, Simon P, Sontheimer T, Leendertz C, Gorka B, Schnegg A, Rech B and Lips K 2012 Influence of deep defects on device performance of thin-film polycrystalline silicon solar cells *Appl. Phys. Lett.* **101** 123904
[14] Boehme C and Lips K 2003 Theory of time-domain measurement of spin-dependent recombination with pulsed electrically detected magnetic resonance *Phys. Rev.* B **68** 245105
[15] Moore E W, Lee S, Hickman S A, Wright S J, Harrell L E, Borbat P P, Freed J H and Marohn J A 2009 Scanned-probe detection of electron spin resonance from a nitroxide spin probe *Proc. Natl Acad. Sci. USA* **106** 22251
[16] Durkan C and Welland M E 2002 Electronic spin detection in molecules using scanning-tunneling-microscopy-assisted electron-spin resonance *Appl. Phys. Lett.* **80** 458
[17] Malissa H, Schuster D I, Tyryshkin A M, Houck A A and Lyon S A 2012 Superconducting coplanar waveguide resonators for low temperature pulsed electron spin resonance spectroscopy arXiv:1202.6305
[18] Narkowicz R, Suter D and Niemeyer I 2008 Scaling of sensitivity and efficiency in planar microresonators for electron spin resonance *Rev. Sci. Instrum.* **79** 084702
[19] Twig Y, Dikarov E, Hutchison W D and Blank A 2011 High sensitivity pulsed electron spin resonance spectroscopy with induction detection *Rev. Sci. Instrum.* **82** 076105
[20] Shtirberg L, Twig Y, Dikarov E, Halevy R, Levit M and Blank A 2011 High-sensitivity Q-band electron spin resonance imaging system with submicron resolution *Rev. Sci. Instrum.* **82** 043708
[21] Twig Y, Dikarov E and Blank A 2013 Ultra miniature resonators for electron spin resonance: sensitivity analysis, design and construction methods, and potential applications *Mol. Phys.* at press, doi:10.1080/00268976.2012.762463
[22] Nickel N H and Schiff E A 1998 Direct observation of dangling bond motion in disordered silicon *Phys. Rev.* B **58** 1114
[23] Poole C P 1983 *Electron Spin Resonance: A Comprehensive Treatise on Experimental Techniques* 2nd edn (New York: Wiley)
[24] Stutzmann M and Biegelsen D K 1983 Electron-spin-lattice relaxation in amorphous-silicon and germanium *Phys. Rev.* B **28** 6256